RESEARCH PAPER

# Inverse analysis determining interfacial properties between metal film and ceramic substrate with an adhesive layer

**Haifeng Zhao · Yueguang Wei**

**Abstract** In the present study, peel tests and inverse analysis were performed to determine the interfacial mechanical parameters for the metal film/ceramic system with an epoxy interface layer between film and ceramic. Al films with a series of thicknesses between 20 and 250 μm and three peel angles of 90°, 135° and 180° were considered. A finite element model with the cohesive zone elements was used to simulate the peeling process. The finite element results were taken as the training data of a neural network in the inverse analysis. The interfacial cohesive energy and the separation strength can be determined based on the inverse analysis and peel experimental result

## 1 Introduction

Due to extensive applications of the thin film/substrate systems in engineering, the researches on the strength, ductility and reliability of these systems have attracted great deal of interest in recent years [1–3]. Thin film delamination is a major failure formation in the thin film/substrate systems [4–8]. Interfacial properties can be characterized by a two-parameter criterion [9–13]. One of the commonly used two-parameter criteria is $(\Gamma_0, \hat{\sigma})$ criterion, where $\Gamma_0$ is the

H. Zhao · Y. Wei (✉)
State-Key Laboratory of Nonlinear Mechanics (LNM),
Institute of Mechanics, Chinese Academy of Science,
Beijing 100080, China
e-mail: Ywei@LNM.imech.ac.cn

interfacial fracture toughness and $\hat{\sigma}$ the adhesion strength. Usually, attention is paid to interfacial fracture toughness (or called cohesive energy) in the elastic case or small-scale yielding case of the 'adherends [2,3,11–17]. When plastic dissipation cannot be neglected, one needs to consider another parameter effect additionally. Figure 1 shows a sketch of the peel test with the film thickness $t$, peel force $P$ and peel angle $\Phi$. The right hand side part of Fig. 1 shows the cohesive zone (CZ) model by which the definition of the interface parameters is given [3–5,8–10,17,18]. There are two important parameters $(\Gamma_0, \hat{\sigma})$ in the CZ model. The determination of $(\Gamma_0, \hat{\sigma})$ for a film/substrate system is the most important goal in the peel test. Through the peel test one can record both the peel force $P$ and the deformation information of the film. From energy balance at the steady-state peeling, one can obtain a relationship between the energy release rate $P(1 - \cos \Phi)$ and the interfacial fracture toughness $\Gamma_0$ as well as the plastic dissipation energy $\Gamma_P$,

$$P(1 - \cos \Phi) = \Gamma_0 + \Gamma_P. \tag{1}$$

In most metal film cases $\Gamma_P$ is a major contribution to the energy release rate $P(1 - \cos \Phi)$. So an appropriate method is needed to determine $\Gamma_0$ when the film deforms plastically [1,3,8–10,15,19–24].

In order to determine $\Gamma_0$ by using the peel test, a beam bending model was adopted in the previous methods [1,3,8–10,15,19–24]. However, this model is only suitable for the cases of the thick film and the weak interface adhesion [22].

In this paper we will focus our attention on the determination of interfacial parameters for thin Al films with thickness ranging from 20 to 250 μm, bonded to a ceramic substrate $(Al_2O_3)$ with a type of epoxy adhesive. Peel tests are performed and a general inverse analysis method based on a neural network is presented to determine the interfacial mechanical parameters. Three cases of peel angles 90°, 135° and 180°
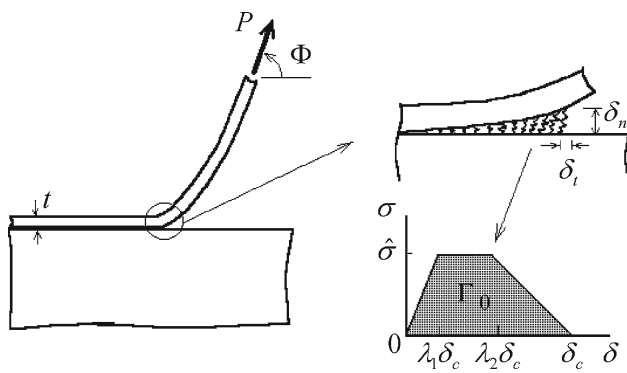
**Fig. 1** Peel test configuration and sketch of cohesive zone model



**Fig. 2** SiO$_2$ spheres used to control the adhesive layer thickness

are considered. In the authors' another paper [25], the interfacial parameters of the Al-film/epoxy/ceramic-substrate were determined through calculating the limit strength of adhesive instead of the inverse analysis. A plane strain FE model with the cohesive zone elements is adopted to simulate the peeling process. The simulation are used as the training data to train a neural network. The trained network is adopted to predict the interfacial cohesive energy $\Gamma_0$ and the separation strength $\hat{\sigma}$.

## 2 Experiments

### 2.1 Overview

Peel tests are performed for the Al films with a series of thicknesses: 20, 50, 80, 100, 200, 225 and 250 microns, bonded to 4.5 mm thick Al$_2$O$_3$ substrates with a type of epoxy/polyimide paste adhesive. The mass ratio of epoxy to polyimide in the adhesive is 1.5. The adhesive shows flexible property in the peel tests.

It is crucial to control the adhesive layer thickness $d$ in preparing the samples. In our peel tests the adhesive layer thickness is kept constant by adding some small SiO$_2$ spheres to the adhesive, see Fig. 2. The adhesive layer thickness is 20 μm in this paper.

All the peel tests are performed using a standard tensile testing machine with a small-scale peel test rig specifically designed for the current research (see Fig. 3). Several peel angles can be easily maintained with this peel test rig. A Questar microscope with long focus is used to observe the crack growth and take micrographs. The thin films are difficult to be fixed directly to the testing machine. So in order to protect the films from tearing, a piece of adhesive tape is used to connect the film to some small metal sheet, and a thin nylon thread is used to connect the metal sheet to the testing machine. Since the nylon thread is about one meter long and the crosshead displacement never exceeds 30 mm, the change of the peel angle during the peel tests is smaller
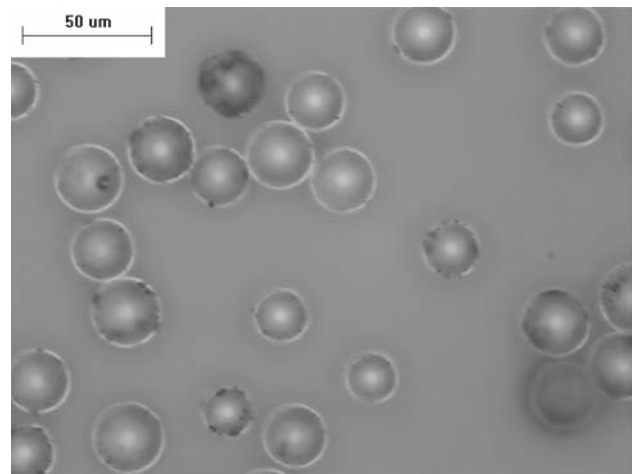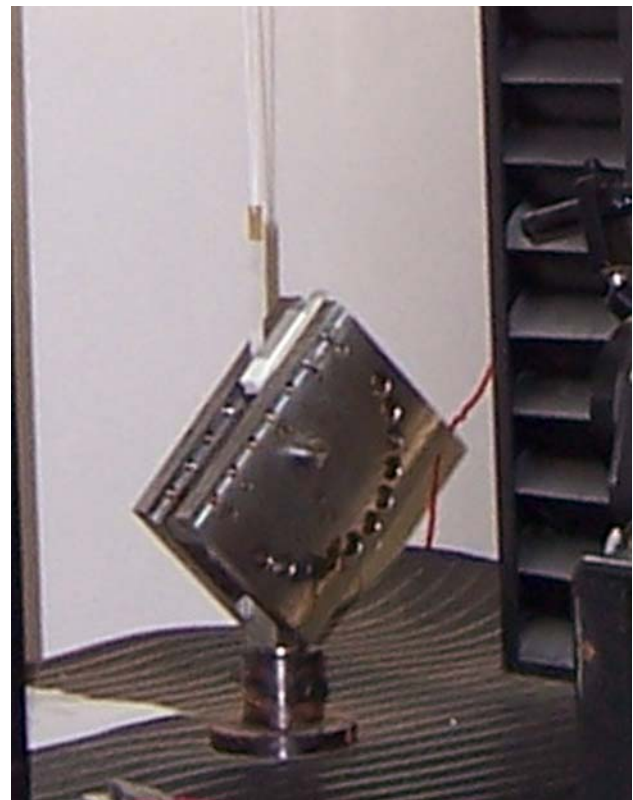


**Fig. 3** Peel test rig made specifically for the current research

than arctg(0.03) $\approx$ 1.5°. Therefore, the peel angle is kept approximately during the peeling process. The peel velocity $v_{crack}$ is kept constant (1 mm/min) during the peeling process, i.e.

$$v/(1 - \cos \Phi) = v_{crack} = \text{const}, \tag{2}$$

where $v$ is the moving velocity of the crosshead and $\Phi$ is the peel angle.

**Table 1** Material parameters of the Al films

| Film thickness/ (μm) | Young's modulus[a]/(GPa) | Poisson ratio[a] | Yield strength/(MPa) | Strain hardening exponent |
| --- | --- | --- | --- | --- |
| 20 | 71 | 0.31 | 36.3 | 0.238 |
| 50 | 71 | 0.31 | 34.0 | 0.243 |
| 80 | 71 | 0.31 | 33.2 | 0.246 |
| 100 | 71 | 0.31 | 32.8 | 0.249 |
| 200 | 71 | 0.31 | 32.0 | 0.251 |
| 225 | 71 | 0.31 | 31.9 | 0.250 |
| 250 | 71 | 0.31 | 31.8 | 0.250 |

[a] From materials handbook

## 2.2 Experimental results

## 2.3 Materials

The Al film is tensed uniaxially and the stress–strain curve is fitted using the following piece power-law hardening relations:

$$\sigma = \begin{cases} E\varepsilon & (\sigma \leq \sigma_y) \\ \dfrac{\sigma_y}{(\sigma_y/E)^n}\varepsilon^n & (\sigma \geq \sigma_y) \end{cases} \qquad (3)$$

where $n$ is the strain hardening exponent. Table 1 shows the fitting material parameters for the Al films.

The substrate material, $Al_2O_3$ is treated as an elastic material with Young's modulus $E = 350\,\text{GPa}$ and Poisson ration $\nu = 0.3$ in the present research.

### 2.3.1 Peel test results

The curves of peel force vs. crosshead displacement are recorded during the peel tests. Figure 4a shows some typical curves of peel force vs. crosshead displacement. From Fig. 4a, the peeling process mainly consists of two stages: initial peeling and steady-state peeling. In the present research, we pay attention to the steady-state peeling.

At least three samples are used to do peel tests for each film thickness and each peel angle. The mean value of the measured steady-state peel forces is taken as a function of the film thickness. The functions are plotted in Fig. 4b. The steady-state peel force increases with increasing film thickness until it reaches the stable value when the film thickness is larger than 200 μm. From Fig. 4b and Eq. (1), the peel angles of 180° and 90° correspond to the maximum and minimum values of plastic dissipation energy among three typical peel angles, respectively, although the larger peel force is needed for 90° than for 135° in the peeling process.

Two typical configurations of the peeled films near the crack tip are shown in Fig. 5a and b for peel angle $\Phi = 180°$ and 135°, respectively. All peeled films are debonded along the interface between the film and the adhesive layer.

For each peel test with $\Phi = 180°$, the curvature radius of the film at the crack tip is also measured by using multiple points to fit the configuration of the film at the crack tip on the micrograph taken by the Questar measuring system, see Fig. 5a. The measured result is shown in Fig. 6.

## 3 FE simulations and neural network inverse analysis

### 3.1 FE model with CZ model

Since the film width (10 mm) in the peel test is much larger than its thickness (20–250 μm), the peel problem can be treated as the plane strain problem. The FE simulation using ABAQUS version 6.5 is performed. Equation (3) is used to characterize the stress–strain relation of the Al film. Large deformation, von Mises yield criterion and isotropic strain hardening will be considered in our FE model. Moreover, for substrate material, since the $Al_2O_3$ substrate undergoes very small deformation during the peel tests, it can treated as an elastic material with Young's modulus $E = 350\,\text{GPa}$ and Poisson ration $\nu = 0.3$.

A single layer of CZ elements [3–5,8–10,15,18] is employed to represent the adhesive layer through adopting double-nodal-number method along interface line. The interface parameters governing the traction separation law are the interface fracture toughness $\Gamma_0$, the separation strength $\hat{\sigma}$, the critical relative displacement at the crack tip $\delta_c = (\delta_n^{c2} + \delta_t^{c2})^{1/2}$, the ratio of critical separation to shear displacements $\delta_n^c/\delta_t^c$ and the shape factors $\lambda_1$ and $\lambda_2$ (see Fig. 1). Earlier studies show that the shape of the traction separation law is relatively unimportant, and two most important parameters are $\Gamma_0$ and $\hat{\sigma}$ [5]. In our FE model, take $\lambda_1 = 0.15$ and $\lambda_2 = 0.5$. The parameter $\delta_n^c/\delta_t^c$ is important in the mixed mode fracture problems, but the predictions are relatively insensitive to this parameter as long as the fracture process is normal-separation dominant [26,27], which is the case for the plastic peeling considered in this paper. So we take $\delta_n^c/\delta_t^c = 1$.

**Fig. 4** **a** Variations of the peel force vs. crosshead displacement. **b** Variations of the steady-state peel force vs. film thickness
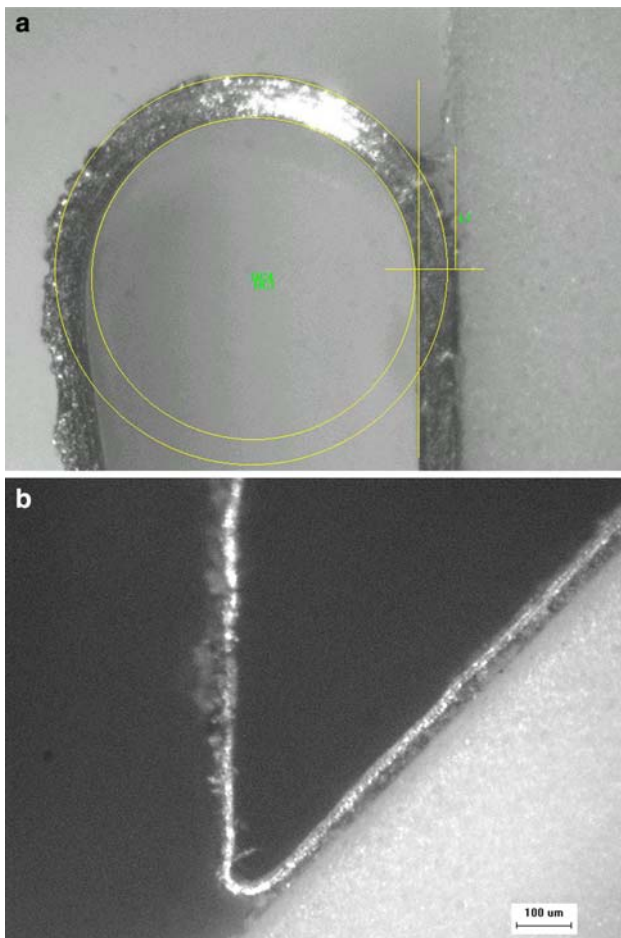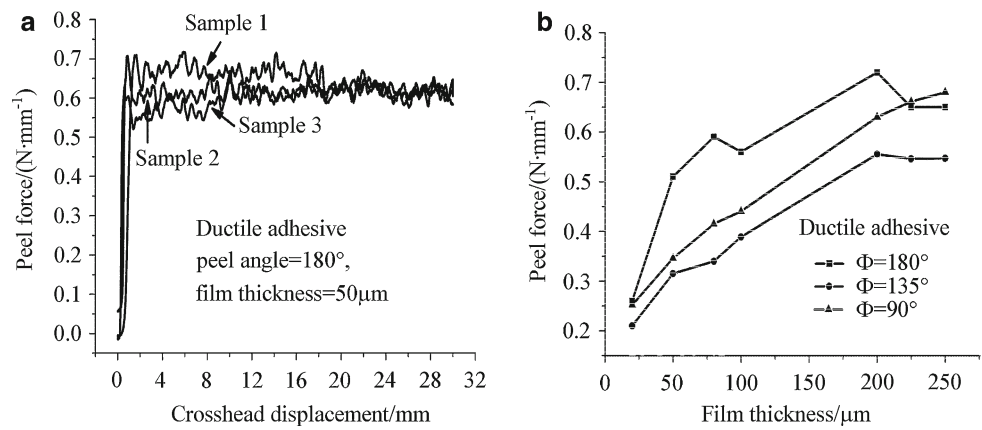




**Fig. 5** **a** Peel angle 180°, film thickness 100 μm; **b** Peel angle 135°, film thickness 20 μm



**Fig. 6** The curvature radius of the film at the crack tip



**Fig. 7** Typical meshes used in the FE calculations

For the convenience of simulating the peeling, a rigid body is settled at the free end of the film. At first the free end of the film is rotated by the peel angle and then the film is peeled along this direction. The film and the substrate are meshed 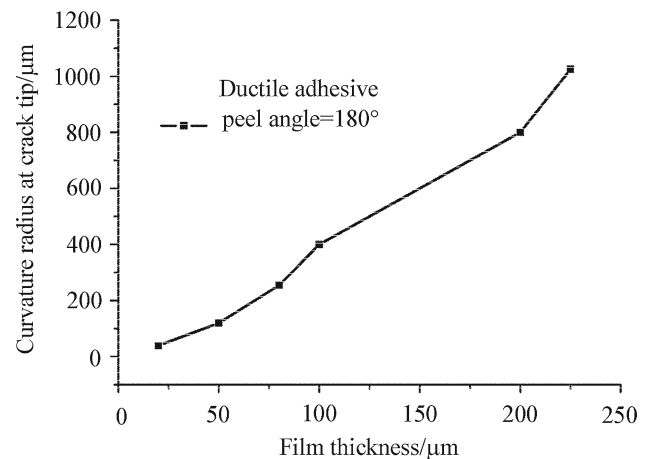by bi-linear rectangular elements with four nodes and four integration points. The film undergoes large bending deformation during the peeling, so at least four layer elements should be divided along the thickness of the film to capture large deformation information. Since Young's modulus of the substrate $Al_2O_3$ is about five times that of the Al film and the substrate undergoes small deformation during the peeling, the sparse meshes are adopted within it. Figure 7 shows the typical meshes used in our FE simulations.

## 3.2 Inverse analysis using neural network to predict $\Gamma_0$ and $\hat{\sigma}$

Since both the interfacial fracture energy $\Gamma_0$ and the separation strength $\hat{\sigma}$ are the most important parameters in the interface fracture researches [5], we selected them as the target to be measured in the present research. Here an inverse analysis is carried out to identify the parameters $\Gamma_0$ and $\hat{\sigma}$ by using the artificial neural network method.

For the film thickness of 50 μm and the peel angle of 180°, both the peel force $P$ and the bending curvature radius $r$ of the film at the crack tip can be described uniquely by the interfacial parameters $\Gamma_0$ and $\hat{\sigma}$,

$$P = f_1(\Gamma_0, \hat{\sigma}), \quad r = g_1(\Gamma_0, \hat{\sigma}). \tag{4}$$

We also have the inverse relations

$$\Gamma_0 = f_2(P, r), \quad \hat{\sigma} = g_2(P, r). \tag{5}$$

Both $f_2$ and $g_2$ can be determined numerically by using the neural network method.

In the inverse analysis based on the neural network method, the finite element solutions are used first as training data to train the neural network. Given a series of values $(\Gamma_0^i, \hat{\sigma}^i)$, one can obtain the same number of values $(P^i, r^i)$ by using the finite element method. The obtained results are used as input data for training the neural network, while values $(\Gamma_0^i, \hat{\sigma}^i)$ are used as target data. From the experimental results shown in Fig. 4b, one can find the region of interfacial fracture energy $\Gamma_0 < 0.2$ N/mm. So for the series $(\Gamma_0^i, \hat{\sigma}^i)$, we take ten values of $\Gamma_0$ in the range (0.02, 0.2) and ten values of $\hat{\sigma}$ in a large range (5, 50). Through finite element calculation, we have 100 values of $(P^i, r^i)$. Comparing the calculated values of $(P^i, r^i)$ and the experimental data for the 50μm thick film with the peel angle of 180° ($P = 0.51$ N/mm, $r = 0.12$ mm), one can find that the true values of $\Gamma_0$ and $\hat{\sigma}$ do fall into the range (0.02, 0.2) and (5, 50), respectively. The neural network can be trained by using $(P^i, r^i)$ and $(\Gamma_0^i, \hat{\sigma}^i)$.

A two-layer feed-forward backpropagation network with two inputs and two outputs is built in MATLAB. There are seven nerve cells in the first layer and the transfer function is TANSIG. The second layer has two nerve cells and the transfer function is PURELIN. TRAINLM is used as the training function for the whole network. The sketch of the neural network is shown in Fig. 8. This network can simulate any function with two dependent and two independent variables, provided that the function is not continuous only at finite points.

The network described in Fig. 8 is trained by using 100 values of $(P^i, r^i)$ and $(\Gamma_0^i, \hat{\sigma}^i)$, noting that these values are based on the finite element calculations. The variations of $g_2$ and $f_2$ based on the neural network method are shown in Figs. 9 and 10, respectively. In these figures, $\Gamma$ and $\sigma$ stand
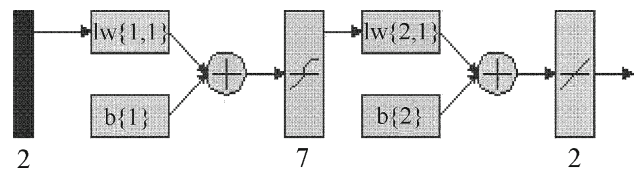


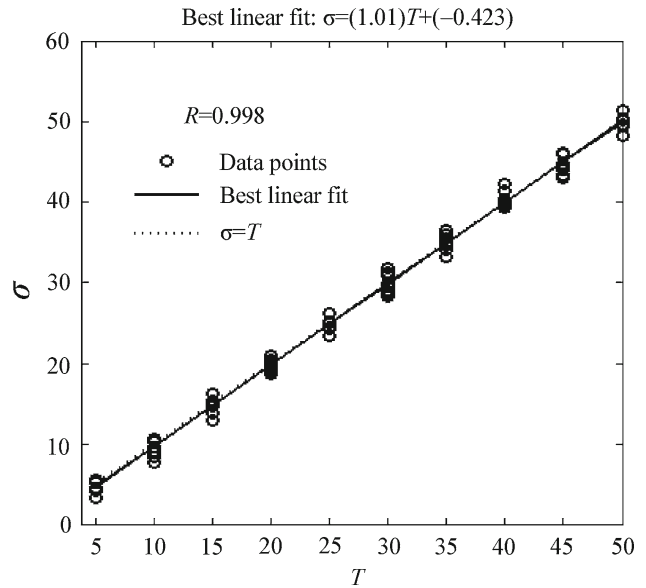**Fig. 8** Sketch of the neural network



**Fig. 9** The effect of simulating $g_2$. Here $\sigma$ is the predicted value by the network with the input data $(P^i, r^i)$, $T$ is the target value and $R = 0.998$ is the correlation coefficient of $\sigma$ and $T$

for the values of $(\Gamma_0, \hat{\sigma})$ to be determined, and $T$ is the target value.

From Figs. 9 and 10, the simulated $f_2$ and $g_2$ by using the trained neural network are accurate. By inputting the experimental data ($P = 0.51$ N/mm, $r = 0.12$ mm) into the trained network, one can obtain, $\Gamma_0 = 0.12$ N/mm, $\hat{\sigma} = 28$ MPa.

### 3.3 Validation of the prediction by the neural network

In order to validate the cohesive parameters obtained in Sect. 3.2, the results of the peel tests with other film thicknesses and peel angles are predicted by the FE model using above determined cohesive parameters. Figure 11 shows the predicted variation of the peel force as a function of the film thickness for various peel angles and the experimental results. It can be seen from Fig. 11 that the FE results agree well with the experimental results. It is found that once the values of $(\Gamma_0, \hat{\sigma})$ are determined in one case of film thickness and peel angle, they could be suitable for other cases of the film thicknesses and peel angles. It seems to conclude that the fracture toughness $\Gamma_0$ and the separation stress $\hat{\sigma}$ can be taken as the intrinsic interfacial parameters which are independent of the film thickness and the peel angle.
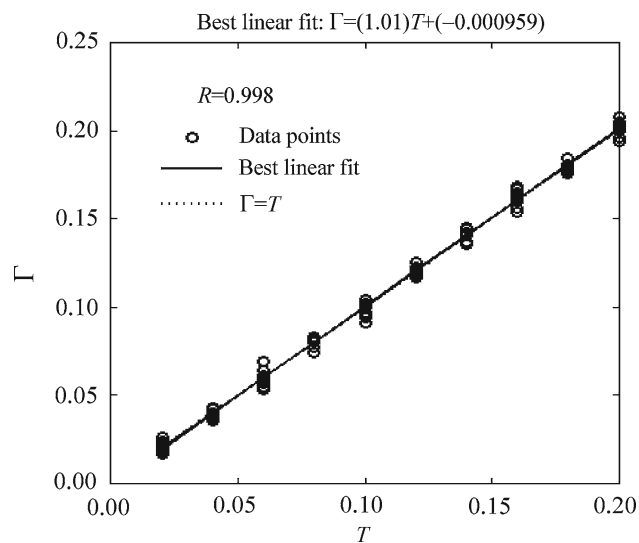
**Fig. 10** The effect of simulating $f_2$. Here $\Gamma$ is the predicted value by the network with the input data $(P^i, r^i)$, $T$ is the target value and $R = 0.998$ is the correlation coefficient of $\Gamma$ and $T$
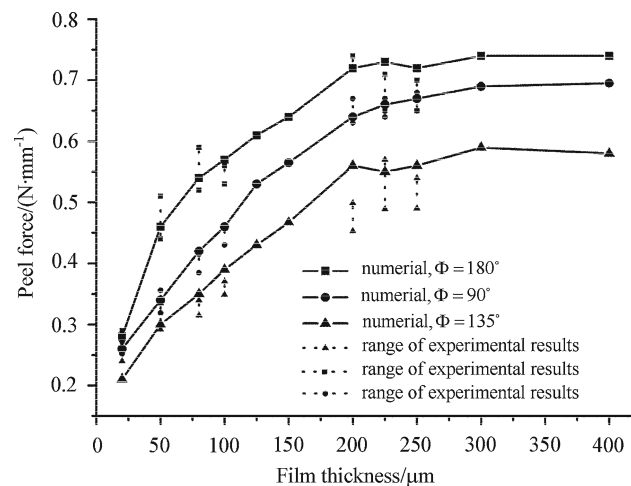


**Fig. 11** The variation of the peel force as a function of the film thickness



**Fig. 12** Configuration of the film at the crack tip, film thickness = 50μm, peel angle = 180°. **a** Film deformation during peeling process from the FE simulation. **b** Film deformation during peeling process from the experiment

Figure 12a shows the simulated configuration of the film at the crack tip. An experimental photograph is shown in Fig. 12b. From the FE simulation, the bending curvature radius $r_1$ of the film at the crack tip is about 116 μm (see Fig. 12a). The range of $r_1$ from experiment is 105–125 μm (see Fig. 12b). The FE model captures both the steady state peeling force and the deformation features of the film.

## 4 Conclusions

Peel tests for the Al film delamination along the ceramic substrate with different peel angles and different film thicknesses are performed. The interface toughness and the separation strength are determined.
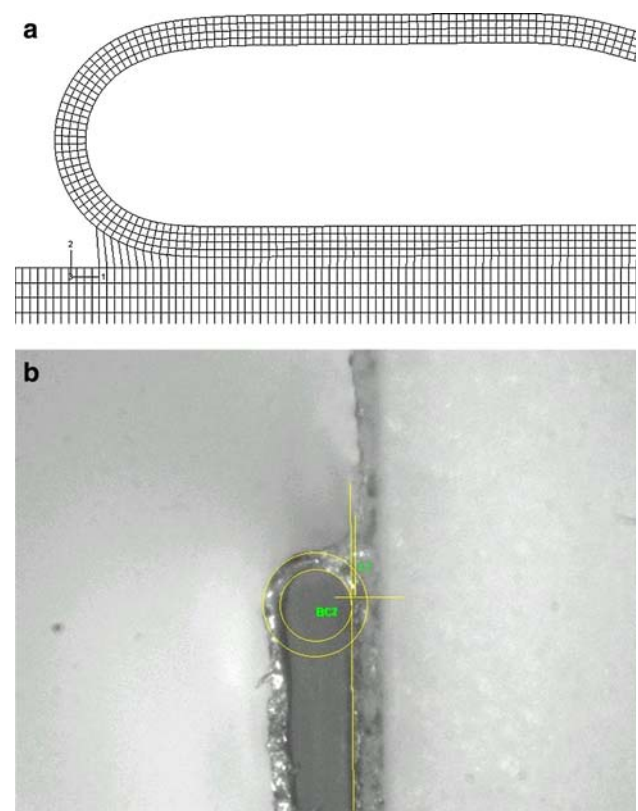
An FE model with the cohesive zone elements is used to simulate the peeling process. The FE results are used to train a neural network. The trained network is adopted to predict the interfacial cohesive energy $\Gamma_0$ and the separation strength $\hat{\sigma}$ for the film/substrate system.

In the present research, we noted that the FE model and the inverse analysis could effectively capture the peeling features for both the steady state peel force and the film deformation. Both the cohesive energy $\Gamma_0$ and the separation strength $\hat{\sigma}$ could be taken as the intrinsic interfacial parameters which are independent of the film thickness and the peel angle.

## References

1. Cotterell, B., Hbaieb, K., Williams, J.G., Hadavinia, H., Tropsa, V.: The root rotation in double cantilever beam and peel tests. Mech. Mater. **38**, 571–584 (2006)
2. Hadavinia, H., Kawashita, L., Kinloch, A.J., Moore, D.R., Williams, J.G.: A numerical analysis of the elastic–plastic peel test. Eng. Fract. Mech. **73**, 2324–2335 (2006)
3. Pardoen, T., Ferracin, T., Landis, C.M., Delannay, F.: Constraints effects in adhesive joint fracture. J. Mech. Phy. Solids **53**, 1951–1983 (2005)

4. Wei, Y.: Thin layer splitting along the elastic–plastic solid surface. Int. J. Fract. **113**, 233–252 (2002)

5. Wei, Y.: Modeling nonlinear peeling of ductile thin films—critical assessment of analytical bending models using FE simulations. Int. J. Solids Struct. **41**, 5087–5104 (2004)

6. Cui, J., Wang, R., Sinclair, A.N., Spelt, J.K.: A calibrated finite element model of adhesive peeling. Int. J. Adhes. Adhesives **23**, 199–206 (2003)

7. Song, J.Y., Jin, Y.: Analysis of the T-peel strength in a Cu/Cr/Polyimide system. Acta. Mater. **50**, 3985–3994 (2002)

8. Yang, Q.D., Thouless, M.D.: Mixed-mode fracture analyses of plastically-deforming adhesive joints. Int. J. Fract. **110**, 175–187 (2001)

9. Yang, Q.D., Thouless, M.D., Ward, S.M.: Numerical simulations of adhesively-bonded beams failing with extensive plastic deformation. J. Mech. Phy. Solids **47**, 1337–1353 (1999)

10. Yang, Q.D., Thouless, M.D., Ward, S.M.: Elastic-plastic mode-II fracture of adhesive joints. Int. J. Solids Struct. **38**, 3251–3262 (2001)

11. Park, I.S., Jin, Y.: An X-ray study on the mechanical effects of the peel test in a Cu/Cr/Polyimide system. Acta Mater. **46**, 2947–2953 (1998)

12. Park, Y.B., Park, I.S., Jin, Y.: Interfacial fracture energy measurement in the Cu/Cr/Polyimide system. Mater. Sci. Eng. A **266**, 261–266 (1999)

13. Asai, H., Iwase, N., Suga, T.: Influence of ceramic surface treatment on peel-off strength between aluminum nitride and epoxy-modified polyaminobismaleimide adhesive. IEEE Trans. Adv. Pack. **24**, 104–110 (2001)

14. Bundy, K., Schlegel, U., Rahn, B., Geret, V., Perren, S.: Improved peel test method for measurement of adhesion to biomaterials. J. Mater. Sci: Mater. Med. **11**, 517–521 (2000)

15. Dillard, D.A., Pocius, A.V.: The mechanics of adhesion. Elsevier, Amsterdam (2002)

16. Lu, Z.X., Yu, S.W., Wang, X.Y., Feng, X.Q.: Effect of interfacial slippage in peel test: theoretical model. Euro. Phys. J. E **23**, 67–76 (2007)

17. Ferracin, T., Landis, C.M., Delannay, F., Pardoen, T.: On the determination of the cohesive zone properties of an adhesive layer from the analysis of the wedge-peel test. Int. J. Solids Struct. **40**, 2889–2904 (2003)

18. Wei, Y., Hutchinson, J.W.: Interface strength, work of adhesion and plasticity in the peel test. Int. J. Fract. **93**, 315–333 (1998)

19. Kim, K.S., Aravas, N.: Elasto-plastic analysis of the peel test. Int. J. Solids Struct. **24**, 417–429 (1988)

20. Kinloch, A.J., Lau, C.C., Williams, J.G.: The peeling of flexible laminates. Int. J. Fract. **66**, 45–70 (1994)

21. Kim, J., Kim, K.S., Kim, Y.H.: Mechanical effects of peel adhesion test. J. Adhe. Sci. Tech. **3**, 175–188 (1989)

22. Wei, Y., Zhao, H., Cao, A.: Modeling and measurement of plastic dissipation in micron-thickness thin film peeling. In: The 12th International Symposium on Plasticity, Halifax, Canada (2006)

23. Moidu, A.K., Sinclair, A.N., Spelt, J.K.: Analysis of the peel test: prediction of adherend plastic dissipation and extraction of fracture energy in metal-to-metal adhesive joints. J. Test. Eval. **23**, 241–255 (1995)

24. Moidu, A.K., Sinclair, A.N., Spelt, J.K.: On the determination of fracture energy using the peel test. J. Test. Eval. **26**, 247–258 (1998)

25. Zhao, H.F., Wei, Y.: Determination of interface properties between micron-thick metal film and ceramic substrate using peel test. Int. J. Fract. **144**, 103–112 (2007)

26. Tvergaard, V., Hutchinson, J.W.: The influence of plasticity on mixed mode interface fracture. J. Mech. Phy. Solids **41**, 1119–1135 (1993)

27. Wei, Y., Hutchinson, J.W.: Nonlinear delamination mechanics for thin Films. J. Mech. Phys. Solids **45**, 1137–1159 (1997)